nature medicine

Activation of Hedgehog signaling by loss of *GNAS* causes heterotopic ossification

Jean B Regard[1,7], Deepti Malhotra[1,7], Jelena Gvozdenovic-Jeremic[1], Michelle Josey[1], Min Chen[2], Lee S Weinstein[2], Jianming Lu[3], Eileen M Shore[4,5], Frederick S Kaplan[4,6] & Yingzi Yang[1]

Heterotopic ossification, the pathologic formation of extraskeletal bone, occurs as a common complication of trauma or in genetic disorders and can be disabling and lethal. However, the underlying molecular mechanisms are largely unknown. Here we demonstrate that $G\alpha_s$ restricts bone formation to the skeleton by inhibiting Hedgehog signaling in mesenchymal progenitor cells. In progressive osseous heteroplasia, a human disease caused by null mutations in *GNAS*, which encodes $G\alpha_s$, Hedgehog signaling is upregulated in ectopic osteoblasts and progenitor cells. In animal models, we show that genetically-mediated ectopic Hedgehog signaling is sufficient to induce heterotopic ossification, whereas inhibition of this signaling pathway by genetic or pharmacological means strongly reduces the severity of this condition. As our previous work has shown that *GNAS* gain-of-function mutations upregulate WNT–β-catenin signaling in osteoblast progenitor cells, resulting in their defective differentiation and fibrous dysplasia, we identify $G\alpha_s$ as a key regulator of proper osteoblast differentiation through its maintenance of a balance between the Wnt–β-catenin and Hedgehog pathways. Also, given the results here of the pharmacological studies in our mouse model, we propose that Hedgehog inhibitors currently used in the clinic for other conditions, such as cancer, may possibly be repurposed for treating heterotopic ossification and other diseases caused by *GNAS* inactivation.

The human skeleton is a complex organ that forms during embryogenesis, grows during childhood, remodels throughout adult life and regenerates following injury. The spatial boundaries of its temporal existence are tightly regulated. Extraskeletal, or heterotopic, ossification occurs sporadically or in several rare genetic disorders[1]. As in normal skeletal morphogenesis, heterotopic ossification can form through either an intramembranous or endochondral process, suggesting that multiple mechanisms are involved[1]. The cellular defect lies in aberrant cell-fate determination of mesenchymal progenitor cells in soft tissues, resulting in inappropriate formation of chondrocytes, osteoblasts or both.

Heterotopic ossification is illustrated by two rare genetic disorders that are clinically characterized by extensive and progressive extraskeletal bone formation: fibrodysplasia ossificans progressiva (FOP) and progressive osseous heteroplasia (POH). In FOP (OMIM 135100), activating mutations in activin receptor type-1, a bone morphogenetic protein type I receptor, induce heterotopic ossification through endochondral ossification[2]. Ectopic bone morphogenetic protein (BMP) signaling induces ectopic chondrocyte differentiation before bone formation, and heterotopic ossification is preceded by ectopic cartilage formation in FOP[3]. However, in POH (OMIM 166350) and Albright hereditary osteodystrophy (AHO, OMIM 103580), heterotopic ossification occurs predominantly through an intramembranous process[4,5], and ectopic osteoblasts differentiate from mesenchymal progenitors independently of chondrocytes in these disorders. Clinically, POH presents during infancy with dermal and subcutaneous ossifications that progress during childhood into skeletal muscle and deep connective tissues (for example, tendons, ligaments and fascia). Over time, ectopic ossifications lead to ankylosis of affected joints and growth retardation of affected limbs. By contrast, ectopic bone formation in AHO presents later in life and is largely restricted to cutaneous and subcutaneous tissue[6].

POH and AHO are caused by inactivating mutations in *GNAS*[4,5,7,8] encoding $G\alpha_s$, which transduces signals from G protein–coupled receptors (GPCRs). However, unlike the case with FOP, the molecular mechanism underlying POH and AHO remains unknown, as the connection between $G\alpha_s$ and a signaling pathway that is both necessary and sufficient to control intramembranous ossification has not been determined.

$G\alpha_s$ has emerged as a seminal regulator of mesenchymal progenitors in the skeletal system. Activating mutations in *GNAS* cause fibrous dysplasia (OMIM 174800), in which osteoblast differentiation from mesenchymal progenitors is impaired[9]. We have found previously that activated Gα proteins have important roles during skeletal development and in disease by modulating Wnt–β-catenin signaling strength[10]. The activating *GNAS* mutations that cause fibrous dysplasia potentiate Wnt–β-catenin signaling, and activation of Wnt–β-catenin signaling in osteoblast progenitors results in

[1]National Human Genome Research Institute, National Institutes of Health, Bethesda, Maryland, USA. [2]National Institute of Diabetes and Digestive and Kidney Diseases, National Institutes of Health, Bethesda, Maryland, USA. [3]Codex BioSolutions, Gaithersburg, Maryland, USA. [4]Department of Orthopaedic Surgery, Perelman School of Medicine at the University of Pennsylvania, Philadelphia, Pennsylvania, USA. [5]Department of Genetics, Perelman School of Medicine at the University of Pennsylvania, Philadelphia, Pennsylvania, USA. [6]Department of Medicine, Perelman School of Medicine at the University of Pennsylvania, Philadelphia, Pennsylvania, USA. [7]These authors contributed equally to this work. Correspondence should be addressed to Y.Y. (yingzi@mail.nih.gov) or J.B.R. (jean.regard@novartis.com).

Received 19 February; accepted 19 July; published online 29 September 2013; corrected online 18 October 2013 (details online); doi:10.1038/nm.3314

a fibrous dysplasia–like phenotype[10]. It is notable that neither POH nor AHO mirrors fibrous dysplasia phenotypically or molecularly. Removal of *Gnas* in mice weakened Wnt–β-catenin signaling and commitment of mesenchymal progenitors to the osteoblast lineage and bone formation[10,11]. Therefore, weak Wnt–β-catenin signaling due to *GNAS* inactivation cannot be the cause of POH or AHO.

$G\alpha_s$ is a physiological activator of protein kinase A (PKA), an inhibitor of Hedgehog signaling that governs a wide variety of processes during development[12–14]. However, Hedgehog signaling has not been found to be required for intramembranous ossification as occurs in POH[15]. In addition, a causal link between $G\alpha_s$ and Hedgehog signaling has never been established in any genetic system[16–18]. Furthermore, although activated $G\alpha_i$ has been implicated in promoting Hedgehog signaling activity in *Drosophila*[19], it is neither sufficient nor necessary for Hedgehog signaling, at least in vertebrates[20,21].

Trauma-associated nonhereditary heterotopic ossification is a common complication in adults[22] and remains a major unresolved medical challenge. Genetic forms of heterotopic ossification provide the opportunity to identify the molecular mechanisms whereby bone formation is spatially restricted. We therefore investigated which molecular pathways regulated by $G\alpha_s$ induce ectopic osteoblast differentiation in animal models of POH.

RESULTS

Loss of *Gnas* leads to POH-like skeletal anomalies

Unlike in patients with POH, heterozygous loss of *Gnas* function in $Gnas^{+/-}$ mice causes osteoma cutis, a cutaneous condition characterized by the presence of bone within the skin through an unknown mechanism, only late in life[23,24]. Because heterotopic ossification in $Gnas^{+/-}$ mice lacks the two critical POH features of early onset and progressive invasion into deep tissues, we hypothesized that elimination of the other allele of *Gnas* was required to achieve this phenotype. Therefore, we completely removed *Gnas* in limb mesenchymal progenitor cells using the *Prrx1-cre* line. Whereas the *Prrx1-cre*; $Gnas^{fl/+}$ mice appeared normal, homozygous loss of *Gnas* in the *Prrx1-cre*; $Gnas^{fl/-}$ or *Prrx1-cre*; $Gnas^{fl/fl}$ mice resulted in numerous skeletal anomalies, as well as severe and progressive heterotopic ossification resembling the phenotypes of POH (**Fig. 1**). *Gnas* was efficiently removed in the limbs, but not in the axial tissue, by *Prrx1-cre* at embryonic day 14.5 (E14.5), as assessed by mRNA expression, gene deletion in the genome and protein levels (**Supplementary Fig. 1a–c**). The *Prrx1-cre*; $Gnas^{fl/-}$ and *Prrx1-cre*; $Gnas^{fl/fl}$ mice showed similar phenotypes and were born with soft tissue syndactyly (webbing between the digits), fused joints and progressive heterotopic ossification in soft tissues (**Fig. 1**). Extraskeletal mineralization was first detected between E16.5 and E17.5, accelerated perinatally and was extensive by postnatal day 4 (P4). We observed heterotopic ossification in the interdigital regions and between radius and ulna, which resulted in bone fusions by P4 (**Fig. 1a**,**b**). Progressive mineralization continued to P20, when most mutant pups died with extensive bone and joint fusions and tendon mineralization (**Fig. 1c**,**d**).

We observed similar heterotopic ossification phenotypes when we removed *Gnas* using either the *Twist2-cre* (here called *Demo1-cre*) or *Tfap2a-cre* (here called *Ap2-cre*) system, in which Cre excises *Gnas* more broadly in mesenchymal tissues outside of the limb (**Supplementary Fig. 2a**,**b**). Therefore, *Gnas* is required in multiple mesenchymal tissues to suppress ectopic mineralization.

To demonstrate that ectopic mineralization is associated with osteoblast differentiation during ossification, we performed von Kossa staining and immunohistochemistry of the early osteoblast marker osterix[25] and the mature osteoblast marker osteocalcin (**Fig. 1e**,**f** and **Supplementary Fig. 2c**). In P4 mutant limbs, von Kossa staining confirmed the presence of extensive mineralization in the *Prrx1-cre*; $Gnas^{fl/fl}$ mice (**Fig. 1e**). We detected osterix-positive and osteocalcin-positive cells in the ectopic bone tissues in both subcutaneous and interdigital regions, where ectopic cartilage was not found (**Fig. 1f** and **Supplementary Fig. 2c**). These data demonstrate that loss of *Gnas* in mesenchymal progenitor cells induces ectopic osteoblast differentiation through a progressive noncartilaginous intramembranous bone formation process. Thus, the *Prrx1-cre*; $Gnas^{fl/-}$ or *Prrx1-cre*; $Gnas^{fl/fl}$ mouse is a model of POH, and one that allows us to investigate the molecular and cellular mechanism of *Gnas* in restricting bone formation.

Loss of *Gnas* promotes ectopic osteoblast differentiation

Because heterotopic ossification often occurs in adults[22], we investigated whether loss of *Gnas* in adult subcutaneous mesenchymal

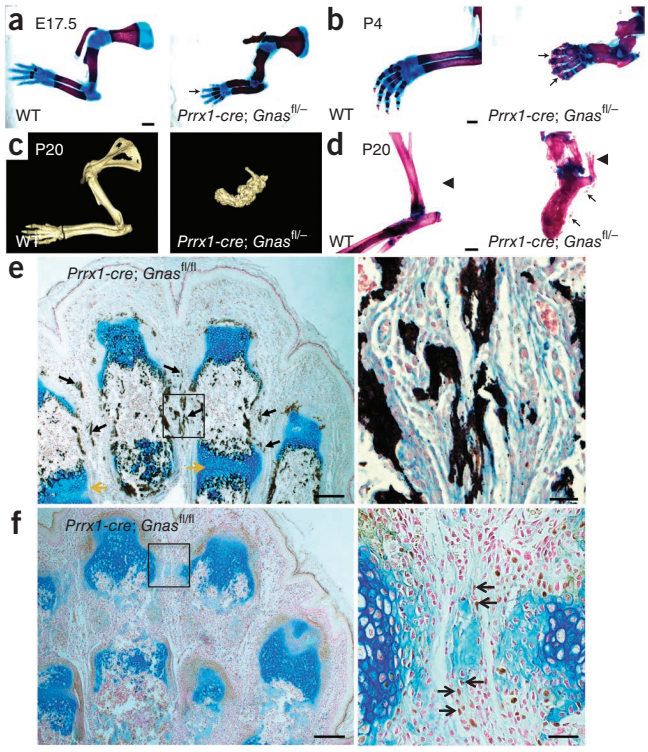

Figure 1 Loss of *Gnas* in limb mesenchyme leads to heterotopic ossification. (**a**,**b**) Representative Alizarin red and Alcian blue staining of forelimbs from wild-type (WT) littermate control and *Prrx1-cre*; $Gnas^{fl/-}$ mutant mice at E17.5 (**a**) and P4 (**b**). Regions of initiating heterotopic ossification (**a**) and overt heterotopic ossification (**b**) are indicated (arrows). Scale bars, 1 mm. (**c**) Representative computed tomography scans of forelimbs from P20 WT littermate and *Prrx1-cre*; $Gnas^{fl/-}$ mutant mice. (**d**) Representative Alizarin red and Alcian blue staining of hindlimbs from P20 WT littermate and *Prrx1-cre*; $Gnas^{fl/-}$ mutant mice. A region of unmineralized Achilles tendon (left) and of ossified Achilles tendon (right) are indicated (arrowheads). Regions of heterotopic ossification are also indicated (arrows). Scale bar, 0.5 mm. (**e**,**f**) Longitudinal sections of the autopod of a P4 *Prrx1-cre*; $Gnas^{fl/fl}$ mouse counterstained with Alcian blue and Sirius red and processed by von Kossa staining (**e**) or by osterix immunohistochemistry (3,3′-diaminobenzidine (DAB), brown) (**f**). Regions of ectopic mineralization (black arrows) and chondrocyte hypertrophy and joint fusion (yellow arrows) are indicated (**e**), as is the brown nuclear staining of osterix-positive cells (black arrows) in interdigital regions of surrounding light-blue stained ossicles (**f**). The boxed interdigital regions in each image are shown in higher magnification on the right. Scale bars, 0.2 mm (left), 0.05 mm (right).

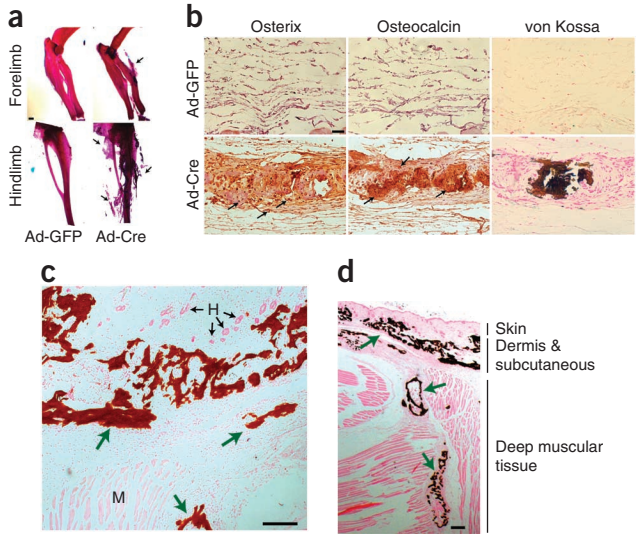

Figure 2 Loss of *Gnas* in adult subcutaneous tissue leads to heterotopic ossification. (**a**) Representative Alizarin red and Alcian blue staining of *Gnas*$^{fl/fl}$ mice injected with either Ad-GFP or Ad-Cre virus in the subcutaneous regions (shown in **Supplementary Fig. 3**). $n = 18$. Extensive ectopic bone formation is indicated (arrows). Scale bar, 1 mm. (**b**) Histological analyses of the ectopic bone formation shown in **a** by osterix and osteocalcin immunohistochemistry (arrows) and von Kossa staining (dark brown). Scale bar, 0.05 mm. (**c**,**d**) Representative von Kossa staining of the ectopic bone (green arrows) in the subcutaneous (**c**) and the deep muscular (**d**) regions in the hindlimbs of *Gnas*$^{fl/fl}$ mice 12 weeks after Ad-Cre virus injection. H, hair follicle; M, muscle. Scale bars, 0.2 mm (**c**), 0.05 mm (**d**).

tissues could also lead to heterotopic ossification. We injected Cre- or GFP-encoding adenoviruses (Ad-Cre or Ad-GFP) subcutaneously into 4-week-old *Gnas*$^{fl/fl}$ mice (**Supplementary Fig. 3**). We detected extensive heterotopic ossification 6 weeks after injection by the presence of ectopic osteoblasts and mineralization in the dermal and subcutaneous regions injected with Ad-Cre but not Ad-GFP (**Fig. 2a**,**b**). This finding demonstrates that loss of *Gnas* in adult subcutaneous mesenchymal tissues is sufficient to cause heterotopic ossification similar to that found in POH and AHO. Notably, as has been found in patients with POH, such induced heterotopic ossification was progressively more severe and invaded deep muscular tissues when more time was allowed for development of heterotopic ossification (**Fig. 2c**,**d**).

To test whether heterotopic ossification results from ectopic osteoblast differentiation of mesenchymal progenitors cells, we isolated bone marrow stromal cells (BMSCs) and subcutaneous mesenchymal progenitors (SMPs) from the *Gnas*$^{fl/fl}$ mice and infected them with Ad-Cre to remove *Gnas*. We observed efficient *Gnas* deletion (**Supplementary Fig. 1d–f**). Ad-Cre–infected BMSCs (**Fig. 3a**,**b**) and SMPs (**Supplementary Fig. 4a**) showed accelerated osteogenic differentiation, as demonstrated by enhanced mineralized matrix formation. This was confirmed by higher expression of osteoblast differentiation markers such as osterix, collagen 1a1, alkaline phosphatase, bone sialoprotein and osteocalcin in BMSCs infected with Ad-Cre compared to those infected with Ad-GFP (**Fig. 3c**).

Gnas is required to inhibit Hedgehog signaling

We have found previously that the activating *GNAS* mutations causing fibrous dysplasia potentiate Wnt–β-catenin signaling[10]. As weak Wnt–β-catenin signaling does not permit osteoblast differentiation[26–29], it is unlikely that *GNAS* inactivation causes ectopic bone formation in POH or AHO by reducing the already diminished Wnt–β-catenin signaling in soft tissue mesenchymal progenitor cells. To test whether $G\alpha_s$ may also regulate bone formation by regulating Hedgehog signaling, we asked first whether $G\alpha_s$ is a major regulator of Hedgehog signaling activity *in vivo* (**Fig. 3d–f**). We found that expression of Hedgehog target genes *Ptch1*, *Gli1* and *Hhip* (which encodes Hedgehog interacting protein) was higher in the *Prrx1-cre*; *Gnas*$^{fl/-}$ limb at E14.5 as compared to control embryos, including in the interdigital areas, before heterotopic ossification appearance at E17.5, indicating that Hedgehog signaling was activated by loss of *Gnas*.

We then asked whether $G\alpha_s$ regulates Hedgehog signaling by regulating PKA. In SMPs and BMSCs lacking *Gnas*, although cAMP levels and PKA activities (assayed by Creb phosphorylation) were also lower compared to control cells containing *Gnas*, Hedgehog signaling was higher, as indicated by expression of *Ptch1*, *Gli1* and *Hhip* (**Fig. 4a–c**). However, Wnt signaling was weaker in the *Gnas*-deficient cells, as indicated by lower expression of the Wnt–β-catenin target genes *Axin2*, *Tcf1* and *Lef1* and β-catenin protein levels[30] (**Supplementary Fig. 4e–f**). *In vivo*, Wnt–β-catenin target gene expression and

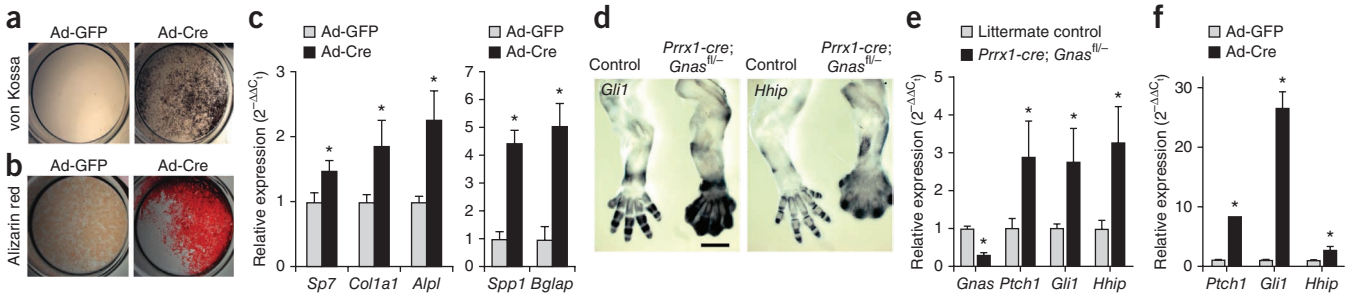

Figure 3 Removal of *Gnas* from mesenchymal progenitor cells upregulates Hedgehog signaling *in vitro* and *in vivo*. (**a**,**b**) Representative von Kossa (**a**) and Alizarin red (**b**) staining of BMSCs from *Gnas*$^{fl/fl}$ mice infected with Ad-Cre or Ad-GFP after 10 d in osteogenic medium. (**c**) Quantitative RT-PCR (qRT-PCR) analysis of osteoblast markers at day 7 following adenovirus infection (mean ± s.d.; $n = 3$; $^*P = 0.017$ for osterix (*Sp7*, also known as *Osx*); $^*P = 0.022$ for collagen 1a1 (*Col1a1*); $^*P = 0.005$ for alkaline phosphatase (*Alpl*); $^*P = 0.003$ for bone sialoprotein (*Spp1*, also known as *Bsp*); $^*P = 0.003$ for osteocalcin (*Bglap*, also known as *Oc*)). (**d**) Representative *in situ* hybridization performed on E14.5 forelimbs from the WT littermate control (left) and the *Prrx1-cre*; *Gnas*$^{fl/-}$ embryos (right). Scale bar, 0.5 mm. (**e**) qRT-PCR analysis of RNA isolated from E14.5 forelimbs. Expression of *Gnas* and transcription targets of Hedgehog pathway is shown (mean ± s.d.; $n = 4$; $^*P = 2.8 \times 10^{-5}$ for *Gnas*; $^*P = 0.012$ for *Ptch1*; $^*P = 0.036$ for *Gli1*; $^*P = 0.01$ for *Hhip*). (**f**) qRT-PCR analysis of Hedgehog pathway target genes in the BMSCs 2–3 d following Ad-Cre or Ad-GFP infection (mean ± s.d.; $n = 3$; $^*P = 1.1 \times 10^{-4}$ for *Ptch1*; $^*P = 0.001$ for *Gli1*; $^*P = 0.007$ for *Hhip*).

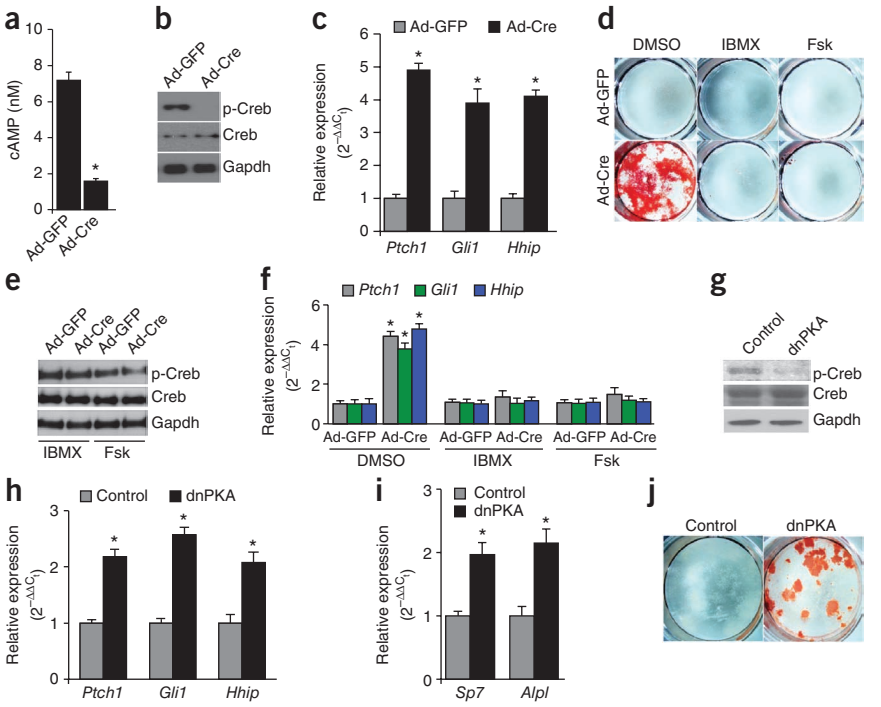

Figure 4 $G\alpha_s$ acts through cAMP and PKA to suppress Hedgehog signaling. (**a**) cAMP levels in SMPs from *Gnas*$^{fl/fl}$ mice as measured 3 d after adenovirus infection (mean ± s.d.; $n = 3$; $^*P = 8.5 \times 10^{-5}$). (**b**) PKA activity indicated by phosphorylated Creb (p-Creb) protein levels in SMPs from *Gnas*$^{fl/fl}$ mice 5 d after adenovirus infection. (**c**) qRT-PCR assay of Hedgehog target gene expression in SMPs from *Gnas*$^{fl/fl}$ mice 5 d after adenovirus infection (mean ± s.d.; $n = 3$; $^*P = 4.4 \times 10^{-4}$ for *Ptch1*; 2.4×10^{-5} for *Gli1*; 2.6×10^{-6} for *Hhip*). (**d**) Alizarin red staining of the SMPs from the *Gnas*$^{fl/fl}$ mice 14 d after the indicated treatment. Fsk, forskolin. (**e**) PKA activity indicated by p-Creb levels in SMPs from the *Gnas*$^{fl/fl}$ mice 5 d after the indicated treatment. (**f**) qRT-PCR assay of Hedgehog target expression in SMPs from the *Gnas*$^{fl/fl}$ mice that had been infected with adenovirus for 7 d and treated as indicated for 5 d (mean ± s.d.; $n = 3$; $^*P = 2.1 \times 10^{-4}$ for *Ptch1*; 8.7×10^{-4} for *Gli1*; 2.6×10^{-4} for *Hhip*). (**g**) PKA activity indicated p-Creb protein levels in WT SMPs infected by dnPKA adenovirus for 5 d. (**h**) qRT-PCR analysis of Hedgehog target gene expression in WT SMPs infected by dnPKA adenovirus for 5 d (mean ± s.d.; $n = 3$; $^*P = 0.001$ for *Ptch1*; 2.1×10^{-4} for *Gli1*; 3.9×10^{-4} for *Hhip*). (**i**) qRT-PCR analysis of osteoblast differentiation marker expression in WT SMPs infected by dnPKA adenovirus for 5 d (mean ± s.d.; $n = 3$; $^*P = 0.003$ for *Sp7* (*Osx*); 4.8×10^{-4} for *Alpl*). (**j**) Alizarin red staining of WT SMP cells infected by dnPKA adenovirus for 14 d.

β-catenin protein levels were lower in the *Prrx1-cre*; *Gnas*$^{fl/-}$ limb at E14.5 as compared to control embryos (**Supplementary Fig. 5a**,**b**). Blocking cAMP degradation with isobutylmethylxanthine (IBMX)[31] or activating cAMP production with forskolin[32] rescued the effects caused by *Gnas* removal (**Fig. 4d–f**). Furthermore, expression of a dominant-negative form of PKA (dnPKA) mimicked the effects of *Gnas* removal (**Fig. 4g–j**). Therefore, $G\alpha_s$ acts through cAMP and PKA to modulate Hedgehog signaling strength.

Regulation of Hedgehog signaling by *Gnas* was further confirmed by strong genetic interactions (i.e., the double mutant phenotype is enhanced compared to either of the single mutants) between *Gnas* and *Ptch1* (**Supplementary Fig. 5c–g**). Ptch1 is an inhibitor of the Hedgehog pathway, and *Ptch1*$^{+/-}$ mice provide a sensitized genetic background to test other suppressors of Hedgehog signaling[33]. *Ptch1* heterozygosity enhanced the phenotypes caused by Dermo1-Cre–induced or Ap2-Cre–induced *Gnas* removal in *Gnas*$^{fl/fl}$ mice (**Supplementary Fig. 5c–g**), indicating that an important *in vivo* function of *Gnas* is suppression of Hedgehog signaling. We further tested this in the developing neural tube, where the Hedgehog signaling gradient patterns the dorsal-ventral axis[34]. In *Gnas*$^{-/-}$ embryos, which died at E9.5, Hedgehog target gene expression was higher compared to that in control embryos, whereas Wnt target gene expression was lower, and the neural tube was ventralized (**Supplementary Fig. 6a–c**). These defects phenocopied mutant embryos resulting from loss of Hedgehog signaling inhibitors such as PKA, Ptch1 and suppressor of fused[13,33,35]. In contrast, inhibiting $G\alpha_i$ family members by expressing pertussis toxin had no effect on limb patterning, skeletal development or Hedgehog signaling activity (**Supplementary Fig. 6d**,**e**). Thus, $G\alpha_s$, but not $G\alpha_i$, is a required *in vivo* regulator of Hedgehog signaling in multiple tissues and at multiple stages of development.

Hedgehog exerts its biological activity by altering the balance between activator (full length) and repressor (truncated) forms of the Gli family of zinc-finger transcription factors (Gli^A and Gli^R, respectively)[36]. Increased Gli^A and reduced Gli^R expression indicate Hedgehog pathway activation[37]. In vertebrates, Gli^R function is largely derived from Gli3, whereas the primary Gli^A activity is mostly from Gli2. Expression of Hedgehog target genes requires Gli^A function. As PKA regulates both Gli3 processing and Gli2 activation[13,38,39], we performed mouse limb bud culture experiments to test whether $G\alpha_s$ acts through PKA to regulate Hedgehog signaling. Whereas a PKA inhibitor, H89, upregulated Hedgehog target gene expression in wild-type limbs (**Supplementary Fig. 7a**), forskolin potently suppressed elevated Hedgehog signaling in the *Prrx1-cre*; *Gnas*$^{fl/-}$ limb (**Supplementary Fig. 7b**). Given that Gli2 is required for ventral neural tube patterning[40,41], expansion of the ventral-most neural tube marker expression in the *Gnas*$^{-/-}$ embryos (**Supplementary Fig. 6c**) indicated that Gli2 is activated by loss of *Gnas*. In addition, full-length Gli3 ($Gli3^A$) and Gli2 levels were higher and $Gli3^R$ levels were lower in the limb bud of *Prrx1-cre*; *Gnas*$^{fl/-}$ mice relative to littermate controls (**Supplementary Fig. 7c**,**d**). Taken together, our data indicate that $G\alpha_s$ suppresses Hedgehog signaling by regulating Gli activation and processing through PKA.

Consistent with this notion, in the limb bud culture we found that cyclopamine, an inhibitor of the Hedgehog receptor Smoothened (Smo)[42], could not suppress Hedgehog target gene expression in *Gnas*-deficient limbs, whereas the Gli inhibitors arsenic trioxide (ATO)[43] and GANT-58 (ref. 44), small-molecule antagonists of Gli transcription factors, could (**Supplementary Fig. 7b**). These results indicate that $G\alpha_s$ acts downstream of Smo and upstream of Gli transcription factors to suppress Hedgehog signaling in embryonic limbs.

Active Hedgehog signaling causes heterotopic ossification

Gli2 mainly functions as a Gli^A that transduces Hedgehog signaling[45,46]. To test whether activated Hedgehog signaling is essential in inducing heterotopic ossification, we removed *Gli2* in *Prrx1-cre*;

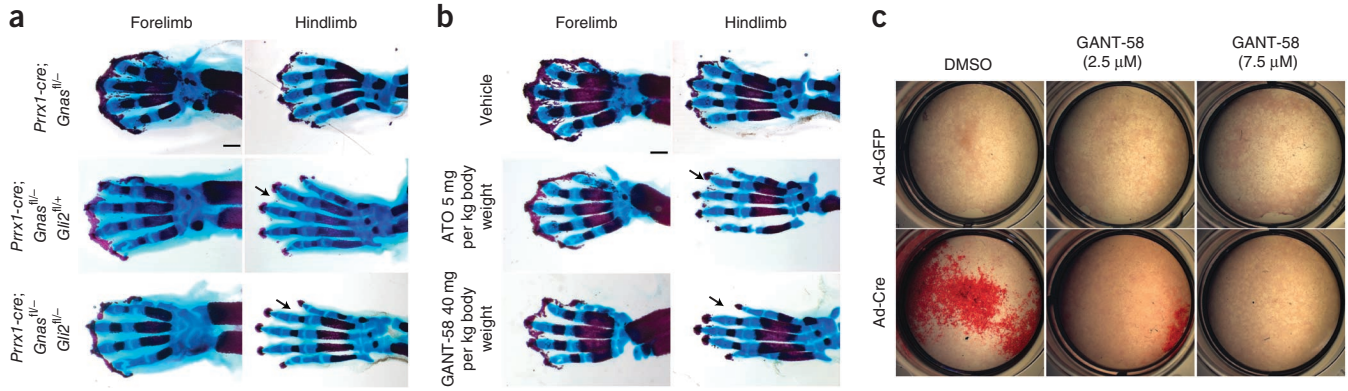

Figure 5 Reducing Hedgehog signaling inhibits heterotopic ossification *in vivo* and *in vitro*. (**a**,**b**) Representative Alizarin red and Alcian blue staining of the limbs from E18.5 embryos with the indicated genotypes. Less severe heterotopic ossification, particularly in the hindlimb, is indicated (arrows). In (**b**), the E18.5 embryos were from the pregnant female mice that had been injected with vehicle or the indicated Hedgehog antagonists three times (E13.5, E15.5 and E17.5). Scale bars, 0.5 mm. (**c**) Alizarin red staining of the differentiating BMSCs from the *Gnas*$^{fl/fl}$ mice with the indicated treatment.

Gnas$^{fl/-}$ mice. Loss of a single copy of *Gli2* led to a partial amelioration of heterotopic ossification in the limbs of *Prrx1-cre*; *Gnas*$^{fl/-}$ mice (**Fig. 5a**). Loss of both copies of *Gli2* further ameliorated ectopic mineralization, particularly in the hindlimb, where the mutant phenotypes of heterotopic ossification, syndactyly and joint fusion were almost completely rescued (**Fig. 5a**). We also achieved amelioration of heterotopic ossification by injecting pharmacologic inhibitors of Gli, ATO or GANT-58 into female mice pregnant with *Prrx1-cre*; *Gnas*$^{fl/-}$ pups (**Fig. 5b**). Whereas higher and more frequent doses of these compounds are required to inhibit Hedgehog-driven tumor growth in adult mice[43,44], similar dosing in pregnant female mice led to spontaneous abortion, precluding their use in this model. In addition to the *in vivo* effect of GANT-58, we also observed inhibition of osteoblast differentiation by GANT-58 *in vitro* in *Gnas*-deficient BMSCs (**Fig. 5c** and **Supplementary Fig. 7e**). Taken together, these data demonstrate that Hedgehog signaling activation is required for osteoblast differentiation driven by loss of *Gnas* function in mesenchymal progenitors.

To test whether Hedgehog signaling is upregulated in patients with POH, we performed GLI1 and GLI2 immunohistochemistry on heterotopic ossification samples from two individuals with POH[7], GLI1 and GLI2 expression was present in hair follicles, where Hedgehog signaling is active under normal conditions (**Supplementary Fig. 7f**,**g**). In the POH samples, GLI1 and GLI2 expression was also present in cells within the ectopic bone tissue (**Fig. 6a–c** and **Supplementary Fig. 7g**). The most intense detection of staining for GLI1 and GLI2 was along the surface of the ectopic bone, suggesting that Hedgehog signaling is most highly upregulated at the leading edge of new bone formation that contains bone-forming progenitor cells. This is consistent with our *in vitro* data showing that Hedgehog signaling is highly upregulated in progenitor cells just before osteoblastic differentiation (**Fig. 3f**). In the limbs of *Prrx1-cre*; *Gnas*$^{fl/fl}$ mice at P4, loss of *Gnas* led to upregulated Gli1 protein expression in most cells compared to the wild-type control (**Supplementary Fig. 8a**). We also found that areas of adipose tissue appeared to contain occasional GLI1-positive cells (**Fig. 6c**), which suggests these cells are

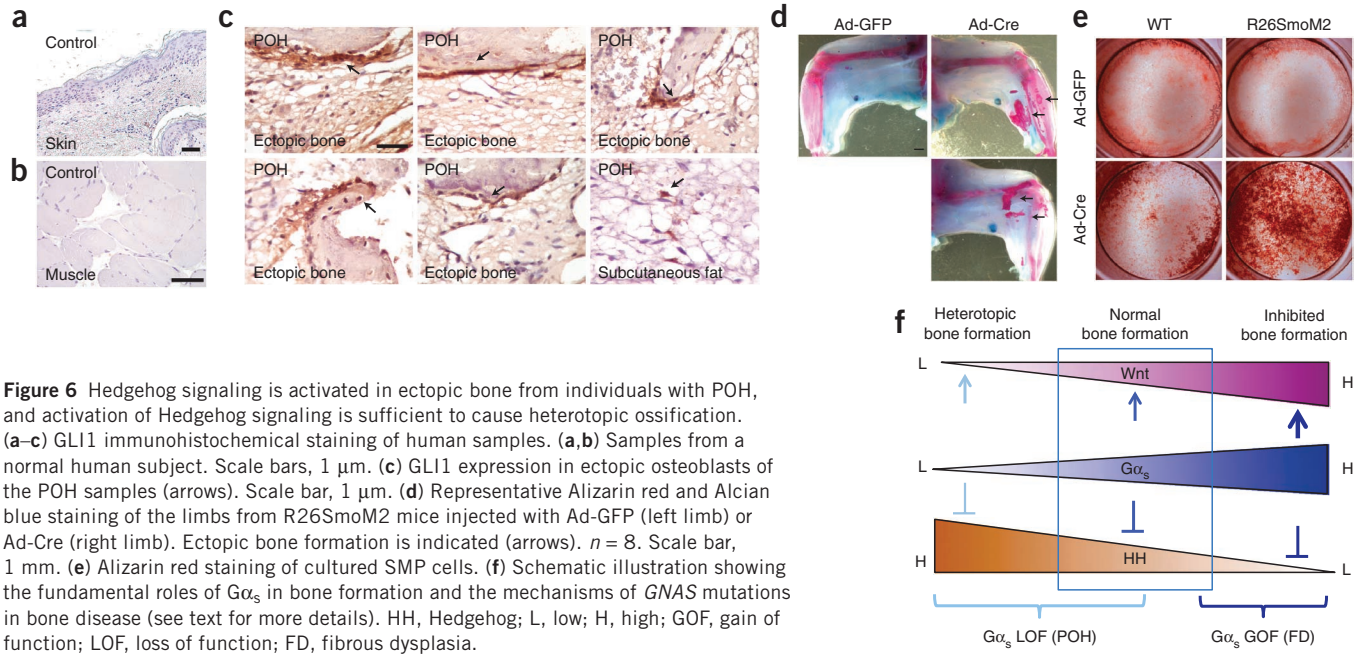

Figure 6 Hedgehog signaling is activated in ectopic bone from individuals with POH, and activation of Hedgehog signaling is sufficient to cause heterotopic ossification. (**a**–**c**) GLI1 immunohistochemical staining of human samples. (**a**,**b**) Samples from a normal human subject. Scale bars, 1 μm. (**c**) GLI1 expression in ectopic osteoblasts of the POH samples (arrows). Scale bar, 1 μm. (**d**) Representative Alizarin red and Alcian blue staining of the limbs from R26SmoM2 mice injected with Ad-GFP (left limb) or Ad-Cre (right limb). Ectopic bone formation is indicated (arrows). $n = 8$. Scale bar, 1 mm. (**e**) Alizarin red staining of cultured SMP cells. (**f**) Schematic illustration showing the fundamental roles of $G\alpha_s$ in bone formation and the mechanisms of *GNAS* mutations in bone disease (see text for more details). HH, Hedgehog; L, low; H, high; GOF, gain of function; LOF, loss of function; FD, fibrous dysplasia.

potential osteoprogenitor cells within the subcutaneous fat tissue. These findings support that upregulated Hedgehog signaling also drives ectopic bone formation in the human disease.

To test whether Hedgehog signaling activation alone is sufficient to cause heterotopic ossification, we injected Ad-Cre subcutaneously into the limbs of the adult R26SmoM2 mice[47], in which an activated form of Smo (SmoM2) is expressed following Cre-mediated recombination. Eight weeks after Ad-Cre injection, but not Ad-GFP injection, we readily detected heterotopic ossification (**Fig. 6d**). BMSCs and SMPs from the R26SmoM2 mice also showed upregulated Hedgehog signaling and accelerated osteoblast differentiation after Ad-Cre infection (**Fig. 6e** and **Supplementary Fig. 8b–d**). These results demonstrate that Hedgehog signaling activation is both necessary and sufficient to induce heterotopic ossification and that Hedgehog signaling must be actively suppressed by $G\alpha_s$ to ensure spatial restriction of bone formation to the normal skeleton.

DISCUSSION

Here we show that loss of *Gnas* causes heterotopic ossification by activating Hedgehog signaling. Further, we provide evidence that previously identified Hedgehog signaling inhibitors, particularly Gli inhibitors that have been developed for cancer therapy, may be repurposed to treat heterotopic ossification and possibly other diseases caused by reduction of $G\alpha_s$ activity. This work, together with our previous study[10], provides deep mechanistic insights into how gain-of-function and loss-of-function mutations of the same *GNAS* gene cause completely different diseases (fibrous dysplasia and POH, respectively) by identifying distinct downstream pathways (Wnt–β-catenin and Hedgehog) that primarily mediate these effects. As both high and low $G\alpha_s$ signaling causes bone diseases, our work highlights the necessity of tightly regulating $G\alpha_s$ activities by GPCRs both spatially and temporally. As there are a large number of GPCRs and their ligands, it would not be surprising that mutations disrupting a single GPCR or the production of one class of GPCR ligands result in less pronounced alteration in Hedgehog or Wnt signaling compared to altered expression of a common downstream effector, such as $G\alpha_s$, and therefore cause less severe phenotypes. Consistent with this, it has been found that loss of a GPCR, Gpr161, which has no known ligand, causes milder developmental defects in mouse embryos[48] compared to those we observed in the *Gnas*$^{-/-}$ mutant embryos in our study.

As a critical regulator of osteoblast differentiation from mesenchymal progenitor cells, $G\alpha_s$ functions by modulating the signaling activities of Wnt–β-catenin and Hedgehog, both of which are key signaling pathways that have fundamental roles in skeletal development and disease[49]. Activation or inactivation of *GNAS* causes upregulation of only one of the two pathways, indicating that one function of $G\alpha_s$ in mesenchymal progenitor cells is to maintain a critical balance between Wnt–β-catenin and Hedgehog signaling, which is required for proper osteogenesis and its spatial regulation. Only appropriate levels of Hedgehog and Wnt signaling, as determined by a specific range of $G\alpha_s$ activities (shown by the box in **Fig. 6f**), result in normal bone formation. Outside the boxed range, extreme Wnt or Hedgehog signaling either inhibits bone formation in the skeleton or causes ectopic bone formation in soft tissues. Therefore, it is likely that distinct mutations in *GNAS* cause corresponding bone diseases such as fibrous dysplasia and POH by altering the balance to enhance either Wnt–β-catenin or Hedgehog signaling, respectively (**Fig. 6f**).

Genetic studies have shown that Wnt signaling acts permissively for osteoblast differentiation. Osteoblast differentiation is favored when Wnt signaling is above a threshold level[26–28,50,51]. Therefore, Wnt signaling alteration itself primarily affects bone formation in the normotopic skeleton and cannot cause ectopic bone formation unless an inducer of osteoblast differentiation is present. Here we identify Hedgehog signaling as one such inducer. In the POH mouse model, lower Wnt signaling was not sufficient to inhibit ectopic bone formation promoted by ectopic Hedgehog signaling. It is important to note that overactivative Wnt signaling also inhibits osteoblast differentiation[10,52–56]. This, together with lower Hedgehog signaling, explains the phenotype of fibrous dysplasia. As both Wnt and Hedgehog signaling pathways have potent regulatory activities, some reduction of their normal signaling levels can be tolerated, whereas ectopic signaling causes deleterious effects. Therefore, the disease phenotypes at the tissue and cellular levels are primarily determined by the pathway that is activated. As Wnt and Hedgehog signaling are both required to regulate a diverse array of developmental and physiological processes, our finding that their balance is regulated by *Gnas* provides a conceptual framework for understanding the molecular and cellular mechanisms of skeletal and possibly other diseases.

Our studies show that ectopic bone in soft tissues forms by differentiation of osteoblast cells from mesenchymal progenitor cells. Even when *Gnas* is removed uniformly in early limb buds, as in the *Prrx1-cre*; *Gnas*$^{fl/-}$ mice, later heterotopic ossification progresses from the distal limb (**Fig. 1**), which contains more progenitor cells than the proximal limb[57,58]. Ligand–mediated Hedgehog signaling is only required for endochondral bone formation[15], raising the possibility that intramembranous bone formation in the skull may be promoted by ligand-independent activation of Hedgehog signaling. Our finding that Hedgehog signaling activation due to loss of $G\alpha_s$ signaling is both necessary and sufficient for heterotopic ossification through the intramembranous mechanism suggests that this signaling crosstalk may also be important in physiological bone formation and homeostasis. For instance, defective GPCR-$G\alpha_s$ signaling may cause impaired development of cranial and clavicle bones. Furthermore, it would be interesting to determine whether the appearance of extraskeletal dermal bone, which is physiologically important in some species, for example, the armadillo, is caused by alteration in the GPCR-$G\alpha_s$-Hedgehog signaling axis during evolution.

The mosaic nature of heterotopic ossification in POH and AHO suggests that the mild elevation of basal Hedgehog signaling in these patients provides a sensitized tissue background for ectopic osteoblast differentiation that occurs when additional Hedgehog signaling or other osteogenic factors are provided by a local microenvironment. For instance, elevated Hedgehog signaling in the hair follicle may trigger heterotopic ossification in the subcutaneous region in patients with POH and AHO.

Nonhereditary forms of heterotopic ossification often contain a mixture of both cartilage and bone. It is possible that the underlying molecular mechanisms of nonhereditary forms of heterotopic ossification are a combination of those underlying POH and FOP. In fact, the developmental program of ectopic chondrogenesis orchestrated by dysregulated bone morphogenetic protein signaling also upregulates Hedgehog signaling at ectopic sites[59]. Therefore, combining Hedgehog inhibitors and the nuclear retinoic acid receptor-γ agonists[60], which block chondrogenesis, may be a promising strategy for POH, as well as common, nonhereditary forms of heterotopic ossification.

METHODS

Methods and any associated references are available in the online version of the paper.

Note: Any Supplementary Information and Source Data files are available in the online version of the paper.

ACKNOWLEDGMENTS

We thank the entire Yang lab for stimulating discussions. We thank J. Fekecs and P. Andre for helping with the data illustration. The work in the Yang and Weinstein labs was supported by the intramural research programs of NHGRI and NIDDK at the US National Institutes of Health (NIH), respectively. We thank R. Caron for his work on the POH lesion histological analyses. The rabbit anti-Gli3 antibody was provided by S. Mackem (NIH NCI), and the dnPKA adenovirus was a gift from C.-M. Fan (Carnegie Institution for Science). The work in the Kaplan and Shore lab was supported by the Progressive Osseous Heteroplasia Association, the University of Pennsylvania Center for Research in FOP and Related Disorders, the Penn Center for Musculoskeletal Disorders (NIH NIAMS P30-AR050950), the Isaac and Rose Nassau Professorship of Orthopaedic Molecular Medicine and NIH NIAMS (R01-AR046831 and R01-AR41916).

AUTHOR CONTRIBUTIONS

J.B.R., D.M. and Y.Y. designed the experiments and analyzed the data. J.B.R., D.M., F.S.K., E.M.S. and Y.Y. wrote the manuscript. J.B.R., D.M., J.G.-J., M.J. and J.L. carried out the actual experiments. F.S.K. saw the patients with POH. F.S.K. and E.M.S. provided the POH samples and carried out the GLI immunohistochemistry on the human samples. M.C. and L.S.W. generated and provided the *Gnas*$^{fl/fl}$ mice.

COMPETING FINANCIAL INTERESTS

The authors declare no competing financial interests.

1. Shore, E.M. & Kaplan, F.S. Inherited human diseases of heterotopic bone formation. *Nat. Rev. Rheumatol.* **6**, 518–527 (2010).
2. Shore, E.M. *et al.* A recurrent mutation in the BMP type I receptor ACVR1 causes inherited and sporadic fibrodysplasia ossificans progressiva. *Nat. Genet.* **38**, 525–527 (2006).
3. Wozney, J.M. *et al.* Novel regulators of bone formation: molecular clones and activities. *Science* **242**, 1528–1534 (1988).
4. Kaplan, F.S., Hahn, G.V. & Zasloff, M.A. Heterotopic ossification: two rare forms and what they can teach us. *J. Am. Acad. Orthop. Surg.* **2**, 288–296 (1994).
5. Eddy, M.C. *et al.* Deficiency of the α-subunit of the stimulatory G protein and severe extraskeletal ossification. *J. Bone Miner. Res.* **15**, 2074–2083 (2000).
6. Trüeb, R.M., Panizzon, R.G. & Burg, G. Cutaneous ossification in Albright's hereditary osteodystrophy. *Dermatology* **186**, 205–209 (1993).
7. Shore, E.M. *et al.* Paternally inherited inactivating mutations of the *GNAS1* gene in progressive osseous heteroplasia. *N. Engl. J. Med.* **346**, 99–106 (2002).
8. Plagge, A., Kelsey, G. & Germain-Lee, E.L. Physiological functions of the imprinted *Gnas* locus and its protein variants $G\alpha_s$ and $XL\alpha_s$ in human and mouse. *J. Endocrinol.* **196**, 193–214 (2008).
9. Riminucci, M., Robey, P.G., Saggio, I. & Bianco, P. Skeletal progenitors and the *GNAS* gene: fibrous dysplasia of bone read through stem cells. *J. Mol. Endocrinol.* **45**, 355–364 (2010).
10. Regard, J.B. *et al.* Wnt/β-catenin signaling is differentially regulated by Gα proteins and contributes to fibrous dysplasia. *Proc. Natl. Acad. Sci. USA* **108**, 20101–20106 (2011).
11. Wu, J.Y. *et al.* $G_s\alpha$ enhances commitment of mesenchymal progenitors to the osteoblast lineage but restrains osteoblast differentiation in mice. *J. Clin. Invest.* **121**, 3492–3504 (2011).
12. Jiang, J. & Struhl, G. Protein kinase A and hedgehog signaling in *Drosophila* limb development. *Cell* **80**, 563–572 (1995).
13. Tuson, M., He, M. & Anderson, K.V. Protein kinase A acts at the basal body of the primary cilium to prevent Gli2 activation and ventralization of the mouse neural tube. *Development* **138**, 4921–4930 (2011).
14. Jiang, J. & Hui, C.C. Hedgehog signaling in development and cancer. *Dev. Cell* **15**, 801–812 (2008).
15. St-Jacques, B., Hammerschmidt, M. & McMahon, A.P. Indian hedgehog signaling regulates proliferation and differentiation of chondrocytes and is essential for bone formation. *Genes Dev.* **13**, 2072–2086 (1999).
16. Bastepe, M. *et al.* Stimulatory G protein directly regulates hypertrophic differentiation of growth plate cartilage *in vivo*. *Proc. Natl. Acad. Sci. USA* **101**, 14794–14799 (2004).
17. Sakamoto, A., Chen, M., Kobayashi, T., Kronenberg, H.M. & Weinstein, L.S. Chondrocyte-specific knockout of the G protein $G_s\alpha$ leads to epiphyseal and growth plate abnormalities and ectopic chondrocyte formation. *J. Bone Miner. Res.* **20**, 663–671 (2005).
18. Sakamoto, H. *et al.* A kinetic study of the mechanism of conversion of α-hydroxyheme to verdoheme while bound to heme oxygenase. *Biochem. Biophys. Res. Commun.* **338**, 578–583 (2005).
19. Ogden, S.K. *et al.* G protein $G\alpha_i$ functions immediately downstream of Smoothened in Hedgehog signalling. *Nature* **456**, 967–970 (2008).
20. Riobo, N.A., Saucy, B., Dilizio, C. & Manning, D.R. Activation of heterotrimeric G proteins by Smoothened. *Proc. Natl. Acad. Sci. USA* **103**, 12607–12612 (2006).
21. Low, W.C. *et al.* The decoupling of Smoothened from $G\alpha_i$ proteins has little effect on Gli3 protein processing and Hedgehog-regulated chick neural tube patterning. *Dev. Biol.* **321**, 188–196 (2008).
22. Vanden Bossche, L. & Vanderstraeten, G. Heterotopic ossification: a review. *J. Rehabil. Med.* **37**, 129–136 (2005).
23. Pignolo, R.J. *et al.* Heterozygous inactivation of *Gnas* in adipose-derived mesenchymal progenitor cells enhances osteoblast differentiation and promotes heterotopic ossification. *J. Bone Miner. Res.* **26**, 2647–2655 (2011).
24. Huso, D.L. *et al.* Heterotopic ossifications in a mouse model of Albright hereditary osteodystrophy. *PLoS ONE* **6**, e21755 (2011).
25. Nakashima, K. *et al.* The novel zinc finger-containing transcription factor osterix is required for osteoblast differentiation and bone formation. *Cell* **108**, 17–29 (2002).
26. Hill, T.P., Spater, D., Taketo, M.M., Birchmeier, W. & Hartmann, C. Canonical Wnt/β-catenin signaling prevents osteoblasts from differentiating into chondrocytes. *Dev. Cell* **8**, 727–738 (2005).
27. Day, T.F., Guo, X., Garrett-Beal, L. & Yang, Y. Wnt/β-catenin signaling in mesenchymal progenitors controls osteoblast and chondrocyte differentiation during vertebrate skeletogenesis. *Dev. Cell* **8**, 739–750 (2005).
28. Hu, H. *et al.* Sequential roles of Hedgehog and Wnt signaling in osteoblast development. *Development* **132**, 49–60 (2005).
29. Holmen, S.L. *et al.* Essential role of β-catenin in postnatal bone acquisition. *J. Biol. Chem.* **280**, 21162–21168 (2005).
30. Logan, C.Y. & Nusse, R. The Wnt signaling pathway in development and disease. *Annu. Rev. Cell Dev. Biol.* **20**, 781–810 (2004).
31. Keely, S.L. Jr., Corbin, J.D. & Park, C.R. On the question of translocation of heart cAMP-dependent protein kinase. *Proc. Natl. Acad. Sci. USA* **72**, 1501–1504 (1975).
32. Seamon, K. & Daly, J.W. Activation of adenylate cyclase by the diterpene forskolin does not require the guanine nucleotide regulatory protein. *J. Biol. Chem.* **256**, 9799–9801 (1981).
33. Goodrich, L.V., Milenkovic, L., Higgins, K.M. & Scott, M.P. Altered neural cell fates and medulloblastoma in mouse patched mutants. *Science* **277**, 1109–1113 (1997).
34. Ribes, V. & Briscoe, J. Establishing and interpreting graded Sonic Hedgehog signaling during vertebrate neural tube patterning: the role of negative feedback. *Cold Spring Harb. Perspect. Biol.* **1**, a002014 (2009).
35. Svärd, J. *et al.* Genetic elimination of Suppressor of fused reveals an essential repressor function in the mammalian Hedgehog signaling pathway. *Dev. Cell* **10**, 187–197 (2006).
36. Ingham, P.W. & McMahon, A.P. Hedgehog signaling in animal development: paradigms and principles. *Genes Dev.* **15**, 3059–3087 (2001).
37. Wang, B., Fallon, J.F. & Beachy, P.A. Hedgehog-regulated processing of Gli3 produces an anterior/posterior repressor gradient in the developing vertebrate limb. *Cell* **100**, 423–434 (2000).
38. Zhang, Q. *et al.* Multiple Ser/Thr-rich degrons mediate the degradation of Ci/Gli by the Cul3-HIB/SPOP E3 ubiquitin ligase. *Proc. Natl. Acad. Sci. USA* **106**, 21191–21196 (2009).
39. Pan, Y., Wang, C. & Wang, B. Phosphorylation of Gli2 by protein kinase A is required for Gli2 processing and degradation and the Sonic Hedgehog-regulated mouse development. *Dev. Biol.* **326**, 177–189 (2009).
40. te Welscher, P. *et al.* Progression of vertebrate limb development through SHH-mediated counteraction of GLI3. *Science* **298**, 827–830 (2002).
41. Matise, M.P., Epstein, D.J., Park, H.L., Platt, K.A. & Joyner, A.L. Gli2 is required for induction of floor plate and adjacent cells, but not most ventral neurons in the mouse central nervous system. *Development* **125**, 2759–2770 (1998).
42. Taipale, J. *et al.* Effects of oncogenic mutations in Smoothened and Patched can be reversed by cyclopamine. *Nature* **406**, 1005–1009 (2000).
43. Kim, J., Lee, J.J., Gardner, D. & Beachy, P.A. Arsenic antagonizes the Hedgehog pathway by preventing ciliary accumulation and reducing stability of the Gli2 transcriptional effector. *Proc. Natl. Acad. Sci. USA* **107**, 13432–13437 (2010).
44. Lauth, M., Bergstrom, A., Shimokawa, T. & Toftgard, R. Inhibition of GLI-mediated transcription and tumor cell growth by small-molecule antagonists. *Proc. Natl. Acad. Sci. USA* **104**, 8455–8460 (2007).
45. Bai, C.B. & Joyner, A.L. Gli1 can rescue the *in vivo* function of Gli2. *Development* **128**, 5161–5172 (2001).
46. Joeng, K.S. & Long, F. The Gli2 transcriptional activator is a crucial effector for Ihh signaling in osteoblast development and cartilage vascularization. *Development* **136**, 4177–4185 (2009).
47. Mao, J. *et al.* A novel somatic mouse model to survey tumorigenic potential applied to the Hedgehog pathway. *Cancer Res.* **66**, 10171–10178 (2006).
48. Mukhopadhyay, S. *et al.* The ciliary G-protein–coupled receptor Gpr161 negatively regulates the Sonic Hedgehog pathway via cAMP signaling. *Cell* **152**, 210–223 (2013).
49. Day, T.F. & Yang, Y. Wnt and hedgehog signaling pathways in bone development. *J. Bone Joint Surg. Am.* **90** (suppl. 1), 19–24 (2008).
50. Joeng, K.S., Schumacher, C.A., Zylstra-Diegel, C.R., Long, F. & Williams, B.O. Lrp5 and Lrp6 redundantly control skeletal development in the mouse embryo. *Dev. Biol.* **359**, 222–229 (2011).

51. Holmen, S.L. *et al.* Decreased BMD and limb deformities in mice carrying mutations in both Lrp5 and Lrp6. *J. Bone Miner. Res.* **19**, 2033–2040 (2004).
52. de Boer, J. *et al.* Wnt signaling inhibits osteogenic differentiation of human mesenchymal stem cells. *Bone* **34**, 818–826 (2004).
53. Cho, H.H. *et al.* Endogenous Wnt signaling promotes proliferation and suppresses osteogenic differentiation in human adipose derived stromal cells. *Tissue Eng.* **12**, 111–121 (2006).
54. Boland, G.M., Perkins, G., Hall, D.J. & Tuan, R.S. Wnt 3a promotes proliferation and suppresses osteogenic differentiation of adult human mesenchymal stem cells. *J. Cell. Biochem.* **93**, 1210–1230 (2004).
55. Chen, Y. β-catenin signaling plays a disparate role in different phases of fracture repair: implications for therapy to improve bone healing. *PLoS Med.* **4**, e249 (2007).
56. Kim, J.B. *et al.* Bone regeneration is regulated by Wnt signaling. *J. Bone Miner. Res.* **22**, 1913–1923 (2007).
57. Cooper, K.L. *et al.* Initiation of proximal-distal patterning in the vertebrate limb by signals and growth. *Science* **332**, 1083–1086 (2011).
58. Roselló-Diez, A., Ros, M.A. & Torres, M. Diffusible signals, not autonomous mechanisms, determine the main proximodistal limb subdivision. *Science* **332**, 1086–1088 (2011).
59. Zhang, D. *et al.* ALK2 functions as a BMP type I receptor and induces Indian hedgehog in chondrocytes during skeletal development. *J. Bone Miner. Res.* **18**, 1593–1604 (2003).
60. Shimono, K. *et al.* Potent inhibition of heterotopic ossification by nuclear retinoic acid receptor-γ agonists. *Nat. Med.* **17**, 454–460 (2011).

ONLINE METHODS

Mice. All mouse experiments were approved by the NIH Institutional Animal Care and Use Committee. Unless specifically noted, mice were a mixture of both males and females, and all mice have been previously described in the literature: *Gnas*$^{fl/fl}$ (ref. 61), *Prrx1-cre* (ref. 62), Dermo1-Cre (ref. 63), Ap2-Cre (ref. 64), *Ptch1*$^{fl/fl}$ (ref. 65), *Gli2*$^{-/-}$ (ref. 66), *Gli2*$^{fl/fl}$ (ref. 67), *Smo*$^{f/fl}$ (ref. 68), R26SmoM2 (ref. 69), Rosa26-PTX (ref. 70) and *Gnaz*$^{-/-}$ (ref. 71).

Human samples. Collection of samples from patients with POH was approved by the Institutional Review Board of the University of Pennsylvania. Informed consent was obtained from all subjects. The samples shown are from two female subjects.

Skeletal preparation (Alizarin red and Alcian blue staining). Embryos were skinned and placed in 100% ethanol overnight. Embryos were then placed in staining solution for 2 d and processed according to standard protocols (50 ml staining solution = 2.5 ml 0.3% Alcian blue, 2.5 ml 0.1% Alizarin red, 2.5 ml 100% glacial acetic acid, 42.5 ml 70% ethanol). Rinsed embryos were then placed in 1% KOH until destained, then placed in 80% glycerol for storage.

von Kossa and Alizarin red staining. Tissue sections were deparaffinized and hydrated in distilled water. We added 5% silver hydrate to slides and then placed them under a 60 W lamp for 1 h. Slides were rinsed three times in distilled water. 5% sodium thiosulfate was added to slides for 5 min. We rinsed slides three times in distilled water. We counterstained slides with nuclear fast red for 5 min. We then rinsed slides three times in distilled water. Slides were dehydrated and cleared in xylene before mounting with Permount. For von Kossa staining of cell cultures, we fixed the cells in 2.5% gluteraldehyde in PBS for 2 h, washed them in distilled water and then stained them with 5% silver nitrate under a 60-W lamp for 1 h. We washed the stained cells in distilled water three times, followed by 5% sodium thiosulfate for 5 min, and then rinsed them in water. For Alizarin red staining of cell cultures, we rinsed cells with PBS and fixed them with 4% paraformaldehyde for 1 h at room temperature. After washing them with water, we stained them with freshly made Alizarin red staining solution (1% Alizarin red in 2% ethanol) for 5 min before we washed them five times with distilled water.

Immunohistochemistry. We deparaffinized and then hydrated tissue sections. We then placed slides into boiling 10 mM citrate, pH 6, for 15 min and room-temperature citrate for 15 min. We placed slides in 3% H_2O_2 in methanol for 15 min, equilibrated slides in PBS with 0.1% Tween-20 (PBS-T), blocked them for 1 h with 5% normal goal serum in PBS-T and applied anti-osterix antibody (1:1,000, Abcam; ab22552) or anti-osteocalcin antibody (1:100, #LS-C42094, LifeSpan Biosciences). We washed slides and detected signal using the anti-rabbit ABC elite kit (Vector Labs; PK-6101) and DAB tablets (Sigma-Aldrich; D4293). We counterstained slides with nuclear fast red and Alcian blue, dehydrated them, cleared them with xylene and mounted them with Permount. For GLI1 immunohistochemistry, following incubation with 1:100 GLI1 antibody (Santa Cruz Biotechnology) overnight at 4 °C, sections were incubated with universal secondary antibody (1:200, Broad Spectrum, Zymed Laboratories) for 25 min at 50 °C and then blocked with Background Buster (American MasterTech) for 30 min and hydrogen peroxide blocking reagent (Lab Vision) for 15 min, both at room temperature. Sections were incubated with streptavidin–horseradish peroxidase (Open Biosystem) for 30 min at 50 °C, and color was developed using DAB (SuperPicTure Polymer; Invitrogen) for 5 min at 37 °C. Adult tissue sections for specific protein immunohistochemistry were counterstained with MasterTech Harris Hematoxylin, and nuclear fast red was used as a counterstain for von Kossa staining. Neonatal tissue sections were counterstained with Alcian blue, followed by Sirius red.

qRT-PCR. We isolated the total RNA first with Trizol (Invitrogen) and then with the RNeasy Kit (Qiagen) with on-column DNase digestion. We generated first-strand cDNA using the iScript cDNA Synthesis Kit (BioRad). qPCR was performed using an ABI7900 light cycler for 40 cycles of 95 °C for 15 s and 60 °C for 60 s. PCR product accumulation was detected using SYBR green (Platimun SYBR Green qPCR SuperMix-UDG; Invitrogen). Primers used for amplification were as follows: actin forward 5′-CAC AGC TTC TTT GCA GCT CCT T-3′ and reverse 5′-CGT CAT CCA TGG CGA ACT G-3′; tubulin forward 5′- CAA CGT CAA GAC GGC CGT GTG-3′ and reverse 5′-GAC AGA GGC AAA CTG AGC ACC-3′; Gα_s forward 5′-GCA GAA GGA CAA GCA GGT CT-3′ and reverse 5′-CCC TCT CCG TTA AAC CCA TT-3′; *Ptch1* forward 5′-CTC TGG AGC AGA TTT CCA AGG-3′ and reverse 5′-TGC CGC AGT TCT TTT GAA TG-3′; *Gli1* forward 5′-GAA AGT CCT ATT CAC GCC TTG A-3′ and reverse 5′-CAA CCT TCT TGC TCA CAC ATG TAA G-3′; *Hhip* forward 5′-GGG AAA AAC AGG TCA TCA GC-3′ and reverse 5′-ATC CAC CAA CCA AAG GGC-3′; osterix forward 5′-CCC ACT GGC TCC TCG GTT CTC TCC-3′ and reverse 5′-GCTBGAA AGG TCA GCG TAT GGC TTC-3′; Col1a1 forward 5′-CAC CCT CAA GAG CCT GAG TC-3′ and reverse 5′-GTT CGG GCT GAT GTA CCA GT-3′; Alp1 forward 5′-CAC GCG ATG CAA CAC CAC TCA GG-3′ and reverse 5′-GCA TGT CCC CGG GCT CAA AGA-3′; BSP forward 5′-TAC CGG CCA CGC TAC TTT CTT TAT-3′ and reverse 5′-GAC CGC CAG CTC GTT TTC ATC C-3′; osteocalcin forward 5′-ACC CTG GCT GCG CTC TGT CTC T-3′ and reverse 5′-GAT GCG TTT GTA GGC GGT CTT CA-3′; *Lef1* forward 5′-TCT CAA GGA CAG CAA AGC TC-3′and reverse 5′-CAC TTG AGG CTT CAT GCA CAT-3′; *Tcf1* forward 5′-ACA TGA AGG AGA TGA GAC CA-3′ and reverse 5′-CTT CTT CTT TCC GTA GTT ATC-3′ and *Axin2* forward 5′-ATG TGT GGA TAC GCT GGA CTT-3′ and reverse 5′-TTC TTG ATG CCA TCT CGT ATG-3′. Relative expression was quantified using the $2^{-\Delta\Delta Ct}$ method[72].

***Gnas* genotyping PCR.** Primers used for PCR amplification of the conditional or mutant alleles were 5′-GAGAGCGAGAGGAAGACAGC-3′, 5′-TCGGGCCTCTGGCGGAGCTT-3′ and 5′-AGCCCTACTCTGTCGCA GTC-3′. 100 ng genomic DNA was PCR amplified (95 °C for 3 min, 35 cycles of 95 °C for 30 s, 62 °C for 45 s and 72 °C for 45 s, 72 °C for 8 min, hold at 15 °C), and we analyzed the PCR product on a 2% agarose gel with ethidium bromide to examine the presence of the ~400-bp conditional allele band or the ~250-bp mutant allele band.

***In situ* hybridization and X-gal staining.** Whole-mount *in situ* hybridization and X-gal staining were performed using standard techniques[73].

Immunoblotting. Immunoblotting was performed using standard techniques. The rabbit anti-Gli3 antibody (1:500) was provided by S. Mackem (NIH/NCI). The antibodies for Gα_s (1:1,000, #sc-55546, Santa Cruz Biotechnology), Creb (1:1,000, #3360R, BioVision), p-Creb (1:1,000, #06-519, Millipore), Gli2 (1:1,000, #AF3635, R&D Systems), Gli1 (1:1,000, #NB600-600, Novus Biologicals), β-catenin (1:500, #9562, Cell Signaling Technology), Gapdh (1:10,000, #G8795, Sigma) and α/β-tubulin (1:1,000, #2148, Cell Signaling Technology) were used according to manufacturer's recommendations.

BMSC and SMP isolation and culture in osteogenic medium. We isolated BMSCs by flushing the bone marrow cavity of 6-week-old mice and plating cells in Alpha-MEM, 20% FBS, 100 U/ml penicillin, 100 μg/ml streptomycin, 2 mM glutamine. Before they reached confluence, cells were infected with either Ad-Cre or Ad-GFP. Upon reaching confluence, cells were switched to osteogenic medium (DMEM, 10% lot-selected FBS, 100 U/ml penicillin, 100 μg/ml streptomycin, 2 mM glutamine, 1×10^{-4} M L-ascorbic acid 2-phosphate and 10 mM β-glycerol phosphate) and cultured for the times previously indicated. Subcutaneous skin tissue containing adipose deposits was removed under sterile conditions and washed in PBS supplemented with 100 U/ml penicillin and 100 μg/ml streptomycin on ice. The tissue was then minced and digested with 1 mg/ml collagenase type I and 0.5% trypsin in 0.1% BSA for 2 h at 37 °C. The digested tissue was centrifuged at 650*g* for 10 min, and the pellet was carefully collected after aspirating off the floating fat depots. After a second centrifugation at 650*g* for 10 min, the cellular pellet was filtered through a 100-μm mesh filter to remove debris. The filtrate was cultured in 100-mm cell culture dishes under the same condition as the BMSCs.

Limb culture. We performed limb culture as described[74]. BGJb culture medium was supplemented with 0.2% bovine serum albumin (Sigma Aldrich) and forskolin (Sigma Aldrich), IBMX (Sigma Aldrich), cyclopamine (BIOMOL),

ATO (Sigma Aldrich) or GANT-58 (Tocris) at the indicated concentrations. Medium was changed every alternate day.

Neural tube analysis. Analysis of neural tube patterning along the dorsal-ventral axis was done as described[75].

cAMP measurement. To measure the cAMP levels in cells, we incubated the the cells in the presence of cAMP stabilizer, IBMX, for 30 min and then trypsinized and flash froze the cells until cAMP measurement. We used the ACTOne cAMP Fluorometric ELISA Kit (#CB-80500-503, Codex BioSolutions) per manufacturer's recommendations.

Arsenic trioxide and GANT-58 treatments. We placed 50 mg of ATO in the bottom of a 50-ml conical tube and dissolved it with 1 ml of 1 N NaOH. 48 ml of PBS was then added to the tube, and 0.82 ml of 1.2 N HCl was added to adjust the pH to 7.2. We dissolved GANT-58 in 20% DMSO and then diluted it with corn oil before injection. We weighed and then injected the pregnant mice with care to avoid injection into the uterus.

GANT-58 cell treatments. BMSCs were grown to confluence and placed in osteogenic medium for 10 d with or without GANT-58 at the indicated concentrations.

Adenovirus injection and treatment. 2 µl of the Cre recombinase or GFP adenovirus from SAIC-Frederick (~1×10^{10} PFU/ml) were diluted in 100 µl PBS solution and injected into the subcutaneous region of the limbs of 4-week-old mice. 6 weeks after injection, the mice were euthanized, and the skins of the limbs were removed. Ectopic bone formation was analyzed by skeletal preparation and histological procedures. For the R26SmoM2 mice, adenovirus injection was performed at 4 weeks of age and analysis was performed at 8 weeks of age.

Adenovirus cell culture treatment. The Cre recombinase and GFP adenoviruses obtained from SAIC-Frederick (~1×10^{10} PFU/ml) was diluted 1:2,000 to infect cells. The dnPKA adenovirus was a gift from C.-M. Fan (~1×10^{10} PFU/ml) and diluted to 1:300 to infect cells.

Statistical analyses. Statistical significance was assessed using two-tailed Student's *t* test for comparisons between two groups or by multivariate analysis of variance for multigroup comparisons. *P* values less than 0.05 were considered significant. Data are presented as mean ± s.d. unless otherwise indicated.

61. Chen, M. *et al.* Increased glucose tolerance and reduced adiposity in the absence of fasting hypoglycemia in mice with liver-specific $G_s\alpha$ deficiency. *J. Clin. Invest.* **115**, 3217–3227 (2005).
62. Logan, M. *et al.* Expression of Cre Recombinase in the developing mouse limb bud driven by a *Prrx1* enhancer. *Genesis* **33**, 77–80 (2002).
63. Yu, K. *et al.* Conditional inactivation of FGF receptor 2 reveals an essential role for FGF signaling in the regulation of osteoblast function and bone growth. *Development* **130**, 3063–3074 (2003).
64. Nelson, D.K. & Williams, T. Frontonasal process-specific disruption of AP-2α results in postnatal midfacial hypoplasia, vascular anomalies, and nasal cavity defects. *Dev. Biol.* **267**, 72–92 (2004).
65. Mak, K.K., Chen, M.H., Day, T.F., Chuang, P.T. & Yang, Y. Wnt–β-catenin signaling interacts differentially with Ihh signaling in controlling endochondral bone and synovial joint formation. *Development* **133**, 3695–3707 (2006).
66. Bai, C.B. & Joyner, A.L. Gli1 can rescue the *in vivo* function of Gli2. *Development* **128**, 5161–5172 (2001).
67. Corrales, J.D., Blaess, S., Mahoney, E.M. & Joyner, A.L. The level of sonic hedgehog signaling regulates the complexity of cerebellar foliation. *Development* **133**, 1811–1821 (2006).
68. Long, F., Zhang, X.M., Karp, S., Yang, Y. & McMahon, A.P. Genetic manipulation of hedgehog signaling in the endochondral skeleton reveals a direct role in the regulation of chondrocyte proliferation. *Development* **128**, 5099–5108 (2001).
69. Mao, J. *et al.* A novel somatic mouse model to survey tumorigenic potential applied to the Hedgehog pathway. *Cancer Res.* **66**, 10171–10178 (2006).
70. Regard, J.B. *et al.* Probing cell type-specific functions of G_i *in vivo* identifies GPCR regulators of insulin secretion. *J. Clin. Invest.* **117**, 4034–4043 (2007).
71. Yang, J. *et al.* Loss of signaling through the G protein, G_z, results in abnormal platelet activation and altered responses to psychoactive drugs. *Proc. Natl. Acad. Sci. USA* **97**, 9984–9989 (2000).
72. Livak, K.J. & Schmittgen, T.D. Analysis of relative gene expression data using real-time quantitative PCR and the $2^{-\Delta\Delta C_T}$ method. *Methods* **25**, 402–408 (2001).
73. Yang, Y., Topol, L., Lee, H. & Wu, J. Wnt5a and Wnt5b exhibit distinct activities in coordinating chondrocyte proliferation and differentiation. *Development* **130**, 1003–1015 (2003).
74. Storm, E.E. & Kingsley, D.M. GDF5 coordinates bone and joint formation during digit development. *Dev. Biol.* **209**, 11–27 (1999).
75. Bai, C.B., Stephen, D. & Joyner, A.L. All mouse ventral spinal cord patterning by hedgehog is Gli dependent and involves an activator function of Gli3. *Dev. Cell* **6**, 103–115 (2004).

doi:10.1038/nm.3314